Elastance Control of a Mock Circulatory System for Ventricular Assist Device Test

Yih-Choung Yu and Sriram Gopalakrishnan

Department of Electrical and Computer Engineering, Lafayette College, Easton, PA 18042, USA

Abstract – A state-feedback controller was designed to simulate the Starling response of the heart in a mock circulatory system (MCS). The controller drives a voice coil actuator (VCA) to follow a reference volume, and thus generate the desired chamber pressure, by using position and speed feedbacks. The reference volume was adjusted according to the maximum ventricular elastance (E_{max}), end-systolic ventricular pressure, and left atrial pressure to respond to load variation in the MCS. The controller was tested in computer simulation by changing the load conditions and E_{max} of the MCS. The MCS along with the controller was able to reproduce human heart function from healthy to sick conditions. A rotary ventricular assist device (VAD) was then introduced in the simulation to test the MCS. The MCS was able to produce a consistent cardiac function even with the presence of the VAD. These results suggest that the new MCS control system is able to simulate the cardiac function for VAD test.

I. Introduction

As heart disease remains a considerable health problem around the world, the development of both equipment and methodologies for its treatment are of great interest and priority. While the heart transplant is the most widely accepted method for dealing with severe cases of the disease, demand for these transplants exceeds the supply available. Thus, ventricular assist devices (VADs) are being developed as alternatives. Indeed, as the reliability and performance of VADs improves, they are becoming increasingly viable for long-term implants in addition to their traditional role as a bridge to native heart transplantation. There are other encouraging signs for the future of VADs – recently several successful rehabilitations of patients using VADs have been reported **Error! Reference source not found.**, implying that the use of such devices is not limited to long-term implantation or as bridge-to-transplant, but also as bridge-to-recovery.

Promising as their future may be, however, there remain many challenges in the development, in particular the performance evaluation of VADs. Testing of the device and its control strategy is usually performed via animal experimentation or the use of mechanical mock circulation loops. There are several disadvantages associated with both methods – animal testing is costly and time-consuming, while most mock circulation loops available to date have limitations in simulating the native heart in response to the load changes due to VAD intervention. This hemodynamic response is very important in assessing VAD performance under various cardiovascular functions, in particular for evaluating the controller of such devices.

The limitations described above originate from the fixed-stroke nature of traditional mock loops, which does not reflect the consistency of the contractual state of the native heart in response to its load changes. Although ventricular elastance, $E_v(t)$, defined by

$$E_v(t) = P_v(t)/[V_v(t) - V_0], \qquad (1)$$

where $P_v(t)$ and $V_v(t)$ are the ventricular pressure and volume and V_0 is the un-stressed volume, is consistent regardless of the load changes to the ventricle [2] and the maximum of $E_v(t)$ (E_{max}) is an appropriate index of the contractile state of the ventricle, controlling the MCS to follow a pre-defined $E_v(t)$ trajectory is limited to a small range of load variation [3,4]. Baloa et al [5] designed a pressure controller that controlled the mock ventricular chamber pressure to track a reference pressure signal, calculated from (1) using the instantaneous volume measurement, $V_v(t)$, while obtaining $E_v(t)$ from a lookup table. However, it was found that preload (the venous pressure) of the MCS was dependent on its afterload (systemic resistance) [6], which was not physiologically meaningful. It was also determined that the robustness of the controller to pressure disturbances, such as introducing a VAD into the MCS, also needed improvement [6].

This paper presents a state feedback position controller to track the chamber volume reference. Unlike a traditional MCS, which was driven to follow a fixed reference either pressure or volume, the reference signal in this MCS was adjusted based on changes in heart rate, E_{max}, end-systolic chamber pressure, and left atrial pressure (as the preload of the MCS). Therefore, this new MCS can better simulate the cardiac hemodynamics in response to load changes. The MCS model, proposed by Baloa et al [5], was adopted with the addition of right atrial compliance and a venous return pumping mechanism for controller design and testing. Performance of the controller was evaluated by changing E_{max}, preload, and afterload. A rotary VAD model [7] was introduced into the MCS to test the robustness of the

controller in response to the VAD intervention. The resulting E_{max}, produced by the MCS with the controller, was consistent regardless of the load changes. This implies that the controller and the MCS should be suitable for use as a VAD test platform.

II. Mock Circulatory System Model

An electrical analogue of the MCS is shown in Fig. 1, where blood pressure, flow, and volume are analogical to voltage, current, and electric charge, respectively. This model was adopted from Baloa et al [5] with the addition of the right atrial compliance (C_{ra}) and the pressure dependent flow (Q_{ra}). The governing equations of the model are listed in (2) to (10). Q_{ra} represents the venous return flow, which is determined by the right atrial pressure in (8) [8]. C_{ra} and Q_{ra} represent a simplified model of the pulmonary circulation in the MCS. These two elements improve the independence of the preload (P_{pv}) from the afterload (R_l), and thus the modified MCS model is a more realistic approximation of the cardiovascular system. Q_{ra} can be implemented in the MCS by regulating the speed of a peristaltic pump to achieve the desired flow rate as determined by (8). The variable x in (4) is the displacement of the voice coil actuator. Table 1 provides the physical meanings and the values of the model parameters. Equation (9) represents the dynamic model of a rotary VAD, where ω_p and Q_p are the rotational speed and blood flow of the VAD, respectively. The values of the VAD model parameters can be found in [7].
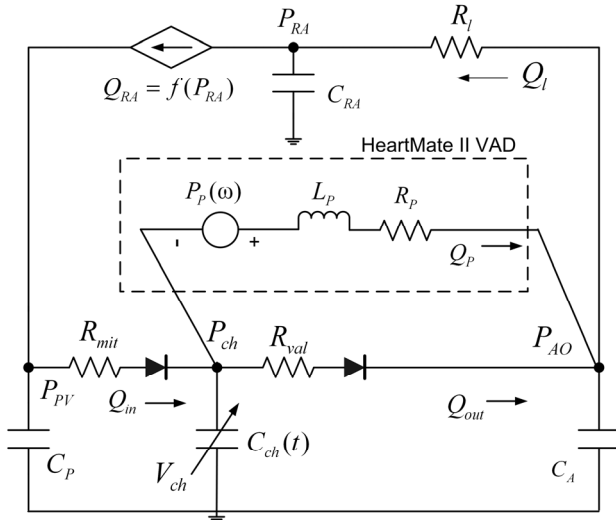

Fig. 1, Electrical analogue of the MCS model with a VAD

$$\dot{P}_{AO} = \left[Q_{out} + Q_P - (P_{AO} - P_{RA}) \ / \ R_l \right]/C_A \quad (2)$$

$$\dot{P}_{PV} = \left(Q_{RA} - Q_{in} \right)/C_P \quad (3)$$

$$\dot{P}_{ch} = \left[Q_{in} + A\dot{x} - Q_{out} - Q_P \right]/C_{ch} \quad (4)$$

$$\dot{P}_{RA} = \left[(P_{AO} - P_{RA}) \ / \ R_l - Q_{RA} \right]/C_{RA} \quad (5)$$

$$Q_{out} = \begin{cases} (P_{ch} - P_{AO}) \ / \ R_{val} & , P_{ch} \geq P_{AO} \\ 0 & , P_{ch} < P_{AO} \end{cases} \quad (6)$$

$$Q_{in} = \begin{cases} (P_{PV} - P_{ch}) \ / \ R_{mit} & , P_{PV} \geq P_{ch} \\ 0 & , P_{PV} < P_{ch} \end{cases} \quad (7)$$

$$Q_{RA} = 240 \cdot [1 - \exp(-\left(P_{RA} + 0.5 \right)/ 3)] \quad (8)$$

$$\dot{Q}_p = \left[k\omega_p^2 - R_p Q_p - (P_{AO} - P_{ch}) \right]/L_p \quad (9)$$

Table 1, Model parameters

Symble	Value (unit)	Description
A	60 (cm^2)	Cross-sectional area of pump-head
f_B	40 (N·s/m)	Frictional coefficient
C_2	100 (cm/m)	Conversion factor
C_1	0.013332 (Pa·cm^2/mmHg·m^2)	Conversion factor
C_A	1.37 (mL / mmHg)	Aortic compliance
C_{ch}	0.1832 (mL/mmHg)	Chamber compliance
C_p	6.74 (mL/mmHg)	Pulmonary venous/Atrial compliance
K_f	27 (N/A)	Current-force factor
K_{sp}	29348 (N/m)	Spring constant
M	0.7533 (kg)	Pump-head mass
R_l	1 (mmHg·s/mL)	Systemic resistance
R_{mit}	0.005 (mmHg·s/mL)	Mitral valve resistance
R_{val}	0.005 (mmHg·s/mL)	Aortic valve resistance
V_0	10 (mL)	Residual chamber volume
V_{bias}	315 (mL)	Maximum chamber volume

III. Controller Design

The control algorithm was designed to produce the reference chamber volume, $V_{ref}(t)$, and drive the voice coil actuator (VCA) to track it. $V_{ref}(t)$ was determined by

$$V_{ref}(t) = (V_{ed} - SV) + SV \cdot v(t_n) , \quad (10)$$

where SV is the stroke volume of the chamber, V_{ed} is the end-diastolic chamber volume, and $v(t_n)$ is a normalized

volume waveform. The normalized time, t_n (defined between 0 and 1), is described by

$$t_n = \begin{cases} t_{s0} \cdot (t/t_s), & 0 \le t < t_s \\ t_{s0} + (1\text{-}t_{s0}) \cdot [(t\text{-}t_s)/(t_C\text{-}t_s)], & t_s \le t < t_C \end{cases} \quad (11)$$

where t_{s0} is the time point at which $v(t_n)$ reaches 0, t_S is the systolic time interval determined by [9]

$$t_S = 0.14 + 0.2 \cdot t_C, \quad (12)$$

and t_C is the cardiac period calculated by $t_C = 60 / HR$. V_{ed} was determined by means of a lookup table from mean left atrial pressure ($\overline{P}_{PV}$), produced by [10]

$$\overline{P}_{PV} = 0.01 \cdot \exp[0.053 \cdot V_{ed}] - 2 \cdot \exp[-0.06 \cdot V_{ed}] \quad (13)$$

Since $E_V(t)$ reaches its maximum value E_{max} near the end of systole [2], the end-systolic chamber volume V_{es} can be derived from (1) as

$$V_{es} = P_{es}/E_{max} + V_0, \quad (14)$$

where P_{es} is the end-systolic chamber pressure. By definition, V_{es} is the difference between the end-diastolic volume, V_{ed}, and the SV, (14) can be written as

$$SV = V_{ed} - P_{es}/E_{max} - V_0 . \quad (15)$$

Since SV in (15) depends on the preload (V_{ed}), afterload (P_{es}) and ventricular contractility (E_{max}), the reference chamber volume obtained from (10) implicitly included the ventricular function in (1).

The mock ventricle was driven by a voice coil actuator. A state-feedback controller, as shown in Fig. 2, was designed to control the VCA to track the reference position signal converted from $V_{ref}(t)$,

$$R(t) = [V_{bias} - V_{ref}(t)] / (A*C_2), \quad (16)$$

where V_{bias} is the maximum chamber volume and C_2 is a unit conversion factor. The dynamics of the VCA can be represented by [5]

$$M\dot{v} = K_f \cdot i - K_{sp} \cdot x - f_B \cdot v - F_l \quad (17)$$

where K_f is the current-force constant and i is the current input to the VCA. K_{sp} is the spring constant, x is the position of the pump-head, f_B is the frictional coefficient

and v is the velocity of the pump head. F_l is the load the VCA produced by the chamber pressure P_{ch},

$$F_l = A \cdot C_1 \cdot P_{ch}, \quad (18)$$

where A is the area of the pump head and C_1 is a unit conversion factor. F_l is non-linear, and can be compensated by adding additional current to the current command sent to the VCA. F_l can therefore be ignored, and the state vector $\underline{X} = [x_1 \ x_2]^T$ can be defined, where $x_1 = x$ and $x_2 = v = \dot{x}$, (17) can be written in a state-space form,

$$\begin{aligned} \dot{\underline{X}} &= \underline{A} \cdot \underline{X} + B \cdot u \\ y &= x = C \cdot \underline{X} \end{aligned} \quad (19)$$

where $\underline{A} = \begin{bmatrix} 0 & 1 \\ -K_{sp}/M & -f_B/M \end{bmatrix}$, $B = \begin{bmatrix} 0 \\ K_f/M \end{bmatrix}$,

$C = \begin{bmatrix} 1 & 0 \end{bmatrix}$, and $u = i$. The pole placement method [11] was used to determine the control gains, $K=[k_1 \ k_2]$ and k_e. Integral control was introduced to improve the steady-state error. Since the VCA velocity v was not measurable, an observer [11] in Fig. 2 was designed to estimate v using the input and output signals.

Assuming that the state estimate $\hat{\underline{X}}$, is equal to the actual state $\underline{X}$, from the block diagram in Figure 2,

$$\begin{bmatrix} \dot{\underline{X}} \\ \dot{x}_N \end{bmatrix} = \underline{A}^* \begin{bmatrix} \underline{X} \\ x_N \end{bmatrix} + \begin{bmatrix} 0 \\ 1 \end{bmatrix} R, \quad (20)$$

where $\underline{A}^* = \begin{bmatrix} 0 & 1 & 0 \\ \dfrac{-K_{sp}-K_f k_1}{M} & \dfrac{-f_B-K_f k_2}{M} & \dfrac{K_f K_e}{M} \\ -1 & 0 & 0 \end{bmatrix}$. By

choosing the desired closed-loop poles at $P_{1,2} = -\zeta \cdot \omega_n \pm j \cdot \omega_n \cdot \sqrt{1-\zeta^2}$ and $P_3 = -10 \cdot \zeta \cdot \omega_n$ [11], where ζ and ω_n are the desired damping ratio and natural frequency of the closed-loop system, the resulting dominator of the closed-loop transfer function is

$$\begin{aligned} \det[sI - \underline{A}^*] &= s^3 + \frac{f_B + K_f k_2}{M} s^2 + \frac{K_{sp} + K_f k_1}{M} s + \frac{K_f K_e}{M} \\ &\equiv s^3 + (12\zeta\omega_n)s^2 + (20\zeta^2+1)\omega_n^2 s + (10\zeta\omega_n^3) \end{aligned} \quad (21)$$
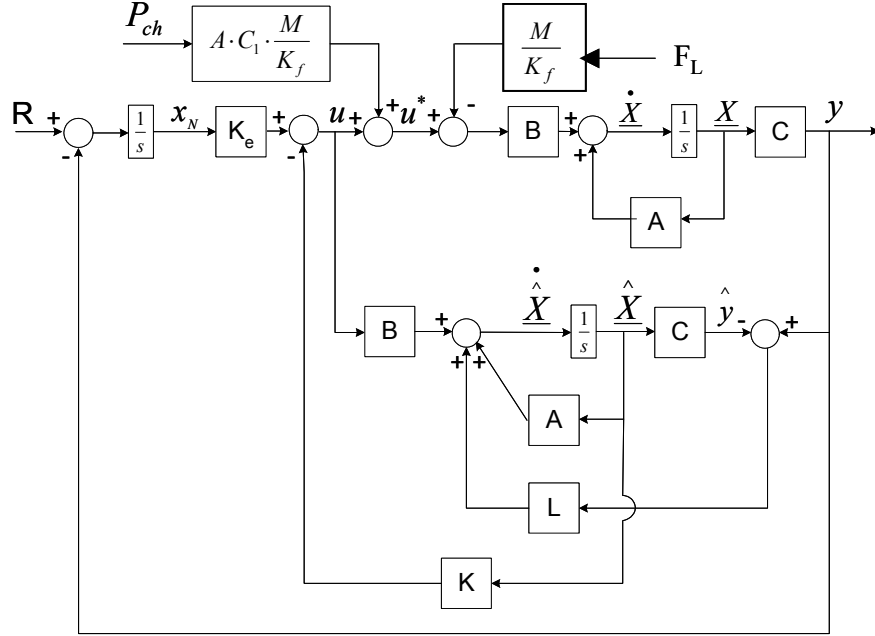
Fig. 2, State space block diagram with observer and correction for steady-state error

The control gains, k_1, k_2, and K_e can be determined by comparing with coefficients in (21) with the settling time and percent overshoot (thus, ζ and ω_n) for the closed-loop system. A 0.02 second settling time and 10% overshoot were chosen in the design so that the phase difference between the reference and actual volume was insignificant over the frequency range of 0.83 to 2.5 Hz, as heart rate of 50 to 150 beats per minute. The resulting control gains are k_1=23010.31, k_2=65.47851, and K_e=3554600.

The chamber pressure, P_{ch}, presents a disturbance, in terms of force F_l, against the VCA pump head. F_l is nonlinear due to the opening and closing of the inlet and outlet valves in the pump chamber. Since the chamber pressure is measurable, additional current can be added to the VCA to compensate F_l. Therefore, the actual current sent into the VCA was

$$U^* = [K_e \cdot \int (R-y) \cdot dt] - K \cdot \hat{\underline{X}} + \frac{M}{K_f} A \cdot C_1 \cdot P_{ch}. \quad (22)$$

Designing the observer entails the choice of an appropriate gain vector, $L=[l_1 \; l_2]^T$, such that the state estimate $\hat{\underline{X}}$ approaches the actual state $\underline{X}$ in a finite time. By choosing the percent overshoot and the settling time for the observer and comparing them with the coefficients in (23) [11],

$$\det[sI - (\underline{A} - LC)] \equiv s^2 + 2\zeta \cdot \omega_n \cdot s + \omega_n^2$$
$$= s^2 + (l_1 + \frac{f_B}{M}) \cdot s + (l_1 \cdot \frac{f_B}{M} + l_2 + \frac{K_{sp}}{M}) \quad (23)$$

The settling time for the observer was 0.001 and the overshoot was 5%. The resulting observer gains are l_1=7946.9 and l_2=25019721.

IV. Controller Testing

Performance of the controller was evaluated in computer simulation. The model of the MCS and the VCA control algorithm was implemented in Simulink (Mathworks Inc., Natick, MA) with the model parameters listed in Table 1. Ventricular contractility and heart rate were set to E_{max}=3.1 and HR=72 to simulate a normal healthy heart. Numerical integration in the model was carried out using Runge-Kutta 4th order method with an integration step size of 1 ms. The simulated pressure waveforms, chamber pressure (P_{ch}), aortic pressure (P_{AO}), right atrial pressure (P_{ra}) and left atrial pressure (P_{PV}), are shown at the top in Fig. 3. Systolic, mean, and diastolic P_{AO} were 113, 97, and 78 mmHg. Mean P_{RA} and P_{PV} were 2.4 and 7 mmHg respectively. The stroke volume was 79 ml/beat as shown at the bottom in Fig. 3, which yielded a cardiac output of 5.69 L/min. These results closely matched the nominal values established by literature [12].

Performance of the MCS to simulate a weak ventricle was evaluated by reducing E_{max} to 60% and 30% of its nominal value, representing mild and severe heart failure, in the tests. Decreasing E_{max} led to the reduction in mean P_{AO} and cardiac output, as well as the elevation of P_{PV} as shown in Table 2. A rotary VAD was then introduced into the simulation to evaluate the MCS and its controller in response to the presence of a VAD. With each E_{max} setting, the rotational speed was set to 8000, 10000, and 12000

revolution per second (rpm). When the simulation reached steady state, mean P_{AO}, mean P_{PV}, cardiac output, and pump flow Q_P were recorded and compared with the clinical data. It can be seen in Table 2 that increasing the VAD speed elevated the mean P_{AO} and reduced the mean P_{PV}. Cardiac output was also increased, boosted by the pump flow Q_P. These results agree with the clinical observations in literature [13].

Table 2, Summary of Hemodynamic Variables from MCS Simulation

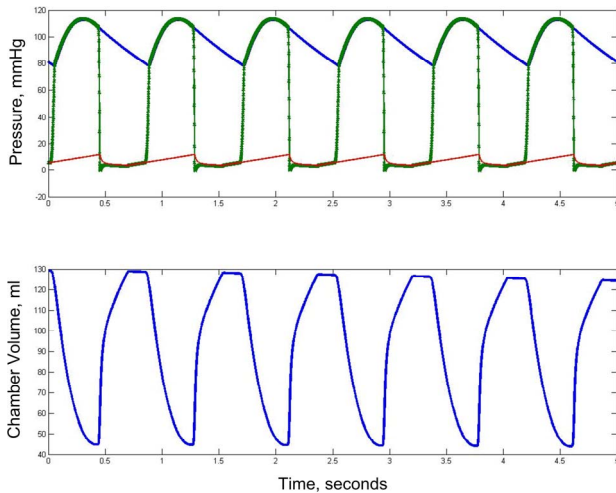| E_{max}	VAD speed	P_{AO} mean	P_{PV} mean	Cardiac Output	Q_P
3.1	-	97	7.04	5.69	-
3.1	8000	100	6.59	5.88	2.57
3.1	10000	117	3.62	6.84	4.44
3.1	12000	137	0.91	8.00	6.89
1.86	-	85	9.07	4.99	-
1.86	8000	92	7,41	5.43	2.71
1.86	10000	114	4.00	6.66	4.49
1.86	12000	137	0.92	7.99	6.90
0.93	-	64	12.68	3.76	-
0.93	8000	84	8.99	4.92	2.83
0.93	10000	109	4.64	6.35	4.59
0.93	12000	136	0.96	7.94	6.93

Fig. 3, Pressure and chamber volume waveforms obtained from the simulation of the MCS with the controller (P_{ch}: green line; P_{AO}: blue line; P_{la}: red line)

V. Validation

The aim of the validation testing was to evaluate the ability of the MCS controller to produce physiologically meaningful waveforms, such as pressure, volume, and flow, in various states of cardiac function ranging from sick to healthy, as well as the presence of VAD. It has been shown experimentally that the cardiac contractility, represented by E_{max}, should be consistent regardless of the load variations presented to the heart [2]. E_{max} is usually obtained from curve fitting using end-systolic pressure and volume data measured by changing the load conditions of the ventricle [5]. This can be explained by (14). Subtracting V_0 and then multiplying E_{max} on both sides of (14) leads to

$$P_{es} = E_{max} \cdot (V_{es} - V_0). \tag{24}$$

End-systolic pressure (P_{es}) and volume (V_{es}) can be changed by varying the load conditions. The slope, obtained from regression using P_{es} and V_{es} data, is the corresponding estimate of E_{max}. The consistency of E_{max} to changing load conditions can be determined statistically by R^2.

In this test, E_{max} in the simulation was set to the same values described before to simulate a healthy, mild failure, and severe failure left ventricle. At each given E_{max}, the output from the venous return pump, Q_{ra}, was gradually scaled from 50% to 150% of its nominal value in (8) to mimic preload changes. The chamber pressure (P_{ch}) and volume (V_{ch}) were recorded to determine P_{es} and V_{es}, and thus the E_{max} estimate. Fig. 4 and 5 depict the test results under normal and failure cardiac function. Both slopes are close to the E_{max} settings with R^2 close to 1, which imply that the MCS with its controller can simulate the cardiac function consistently regardless of the load changes.
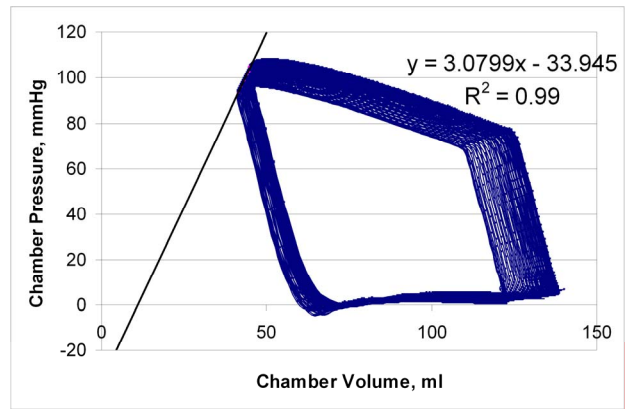

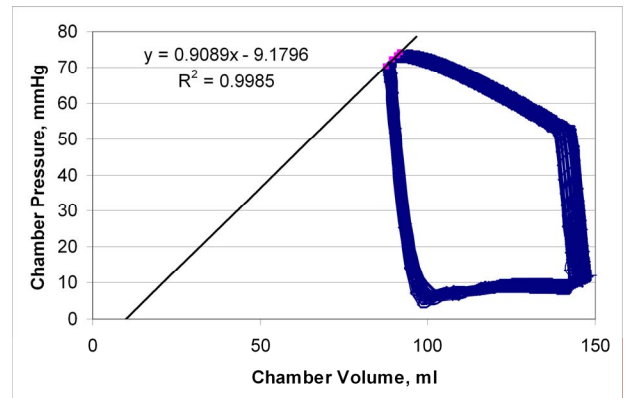Fig. 4, PV Loops of a 100% E_{max} with changing preload

Fig. 5, PV Loops of 30% E_{max} with changing preload

The validation tests with the failure heart were repeated with the presence of VAD support. With each cardiac function setup, the pump was operated at 8000 and 12000 rpm. The test results are summarized in Table 3. The E_{max} estimates (Slope) were still close to the set values with R^2 close to 1. Fig. 6 illustrates the pressure-volume loops of a mild failure heart with VAD operated at 8000 rpm.

Table 3, Summary of the validation tests

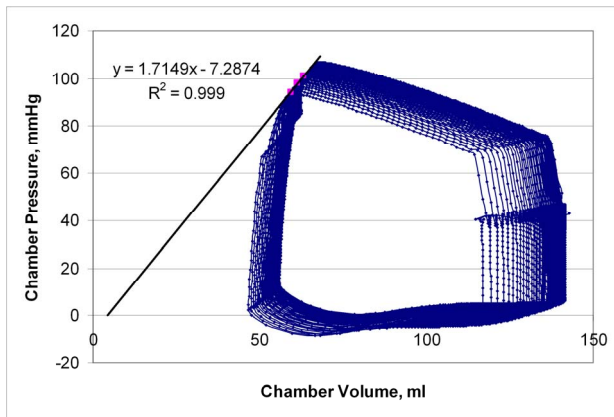| E_{max} Setting	Pump Speed	Slope	Error	R^2
No VAD Support				
3.1	-	3.08	-0.6%	0.99
1.86	-	1.94	4.3%	0.99
0.93	-	0.91	-2.2%	0.99
With VAD Support				
1.86	8000	1.71	-8.1%	0.99
1.86	12000	2.08	11.8%	0.99
0.93	8000	0.90	-3.2%	0.99
0.93	12000	0.96	3.2%	0.99

Fig. 6, PV Loops of 60% E_{max} under VAD support at 8000 rpm with changing preload

VI. Conclusions

A state feedback controller was designed to control a mock circulatory system to produce physiologically meaningful pressure, volume, and flow waveforms based on the contractile state of the left ventricle. A volume reference was generated based on the load conditions (V_{ed} and P_{es}) and contractility (E_{max}) of the mock ventricle. This reference was successfully used to drive a VCA. Performance of the design was evaluated by computer simulation. The MCS was able to generate the key hemodynmic waveforms of healthy and failure cardiac functions. When a VAD model was incorporated with the MCS in simulation, the changes in the hemodynamic variables agreed with those from clinical observations. A series of validation tests showed that the system could produce a consistent E_{max} ($R^2 \approx 1$) for both healthy and failure heart conditions regardless of load

changes as well as the presence of the VAD. This system remains to be tested when a physical realization becomes available.

References

[1] D. J. Ferrar et al., "Long-term follow-up of thoratec ventricular assist device bridge-to-recovery patients successfully removed from support after recovery of ventricular function," *J. Heart Lung Transplant*, vol. 21, no. 5, pp. 516–521, May 2002.

[2] Klabunde, R. *Cardiovascular Physiology Concepts*, Lippincott Williams & Wilkins, Philadelphia, 2005.

[3] Woodard, J.C.; Rock, S.M.; and Portner, P.M. "A sophisticated electromechanical ventricular simulator for ventricular assist system testing," *ASAIO Trans.*, 1991, pp. 210-11.

[4] Williams, J.L.; Antaki, J.F.; Boston J.R.; Williams, S.L.; Woodard, J.C.; Miller, P.J.; and Kormos, R.L. "Load sensitive mock circulatory system for ventricular assist device controller evaluation and development," *Proc. of the 16th Annual Intern. Conf. of the IEEE EMB Society*, 1994, pp. 89-90.

[5] Baloa, L.A.; Boston, J.R.; and Antaki, J.F. "Elastance-based Control of a Mock Circulatory System," *Annals of Biomedical Engineering*, v. 29. 2001. pp. 244 – 251

[6] Loh, Matthew. Modeling and Simulation of a Mock Circulatory System. *Proceedings of the National Conference on Undergraduate Research*. 2003.

[7] Choi, S., et al., "Modeling and identification of an axial flow blood pump," *Proceedings of the American Control Conference*, 1997, pp 3714-3715.

[8] Cavalcanti, S. and Di Marco, L. "Numerical Simulation of the Hemodynamic Response to Hemodialysis-Induced Hypovolemia," *Artificial Organs*, 1999, pp. 1065 – 67.

[9] Rideout, V. *Mathematical Modeling and Computer Simulation of Physiological Systems*, Prentice Hall, Inc., 1991.

[10] Ferrari, G.; De Lazzari, C.; Mimmo, R.; Tosti, G; and Ambrosi, D. "A modular numerical model of the Cardiovascular System for Studying and Training in the Field of Cardiovascular Physiology," *J. of Biomed. Eng.*, 1992, pp. 91-107.

[11] Nise, N.S. Control System Engineering, 5th Ed., John Wiley & Sons, Inc. 2008.

[12] Guyton, A.C. and Hall, J.E. *Textbook of Medical Technology*, 11th Ed., W. B. Saunders Company, 2005.

[13] Xu, L., et al., "Computer Modeling of Interactions of an Electric Motor, Circulatory System, and Rotary Blood Pump," *ASAIO Journal*, 2000, pp. 604-611.